Impact of Fuel-Cladding Bonding on the Response of High Burnup Spent Fuel Subjected to Transportation Accidents

William Lyon[1], Anh Mai[1], Wenfeng Liu[1], Nathan Capps[2]
Joe Rashid[1], Albert Machiels[2], Keith Waldrop[2]

[1]*Nuclear Fuel Technology Division, Structural Integrity Associates, Inc., San Diego, CA 92121 USA*
[2]*Electric Power Research Institute, Palo Alto, CA 94304 USA*
+1 858-455-6350 blyon@structint.com

Abstract. Detailed knowledge of hydrides reorientation, from the circumferential to the radial direction, during dry storage is needed to determine its impact on cladding integrity during transportation and handling accidents. Hydrides reorientation depends directly on the hoop stress, which in turn is dependent on the rod internal pressure, the conditions of the fuel cladding interface, and the manner in which the gas pressure is transmitted through the fractured fuel matrix to the cladding. There is prevalent information, illustrated by numerous radiographs and the often-encountered difficulties in defueling fuel rods, to indicate that fuel-cladding bonding dominates the configuration of high burnup spent fuel rods. In the presence of fuel-cladding bonding, there is no pellet-cladding gap to allow the cladding to deform freely as a pressurized empty tube, and the gas pressure is transmitted to the cladding indirectly, through fragmented material. Under such conditions, cladding deformations become highly constrained, and the cladding hoop stress evolves though complex interaction of the fuel fragments with the cladding. This can lead to a hoop stress that is a fraction of the value calculated by the simple pressurized-tube formula, and potentially below the hydride reorientation threshold. A numerical evaluation of the effect of pellet-cladding bonding on cladding hoop stress, considering variations of fuel cracking patterns and partial bonding configurations, is the subject of this paper.

Keywords: Spent fuel, bonded, cracking, cladding stress distribution

INTRODUCTION

There is prevailing evidence to indicate that sustained constant power operation under high burnup conditions leads to fuel-cladding bonding brought upon by a phenomenon called diffusion welding [1]. Fission products release and oxygen diffusion to the pellet-cladding interface causes the formation of layers of (U, Zr)O_2 at the pellet surface and a ZrO_2 layer at the cladding inner surface. These layers form tenacious bonds between the fuel pellets and the cladding where, as shown by experience, significant mechanical effort has had to be applied during the defueling of high-burnup fuel rods in preparation for post irradiation examination. This bonding condition, which develops under high-burnup (>45 GWd/MTU) operation, becomes a pre-existing condition for spent fuel storage and transportation. As such, it defines the initial conditions for the cladding stresses and the consequential formation of radial hydrides during dry storage.

The prevailing approach of determining the magnitude of cladding hoop stress, which governs the formation of radial hydrides during dry storage, is to use the pressurized empty-tube formula. This open gap assumption has been the basis in all previous studies of characterizing hydrides reorientation conditions at the end of dry storage, including the experimental studies conducted at Argonne National Laboratories which resulted in the development of a cladding ductility criterion in terms of a ductile-brittle transition temperature (DBTT) [2]. However, the pressurized empty-tube formula does not apply to bonded fuel, hence the need for a new approach, as pursued in the present investigation.

At discharge burnup, typically higher than 60 GWd/MTU rod average, the cladding can have a cladding-thickness-average hydrogen concentration that varies with the type of alloy, for example, 500-600 ppm for Zry-4 cladding to less than half that for M5 cladding. At cladding operating temperature, typically in the range 300-320°C, about 100ppm of the hydrogen is in solid solution; the rest is in the form of zirconium hydride platelets predominantly oriented in the circumferential direction. When the spent fuel is transferred from wet storage to dry storage casks

and subjected to vacuum drying temperatures of up to the regulatory limit of 400°C [3], the solid-solution hydrogen concentration rises to about 210 ppm. This amount of hydrogen becomes available for precipitation during the slow cooling of the cladding while in dry storage casks. This precipitation process results in part of the precipitating hydrides to be oriented radially, the fraction depending upon the cladding hoop stress and the vacuum-drying temperature; the higher the vacuum drying temperature, the lower the stress needed to cause hydrides re-orientation, as shown in Figure 1 [4].

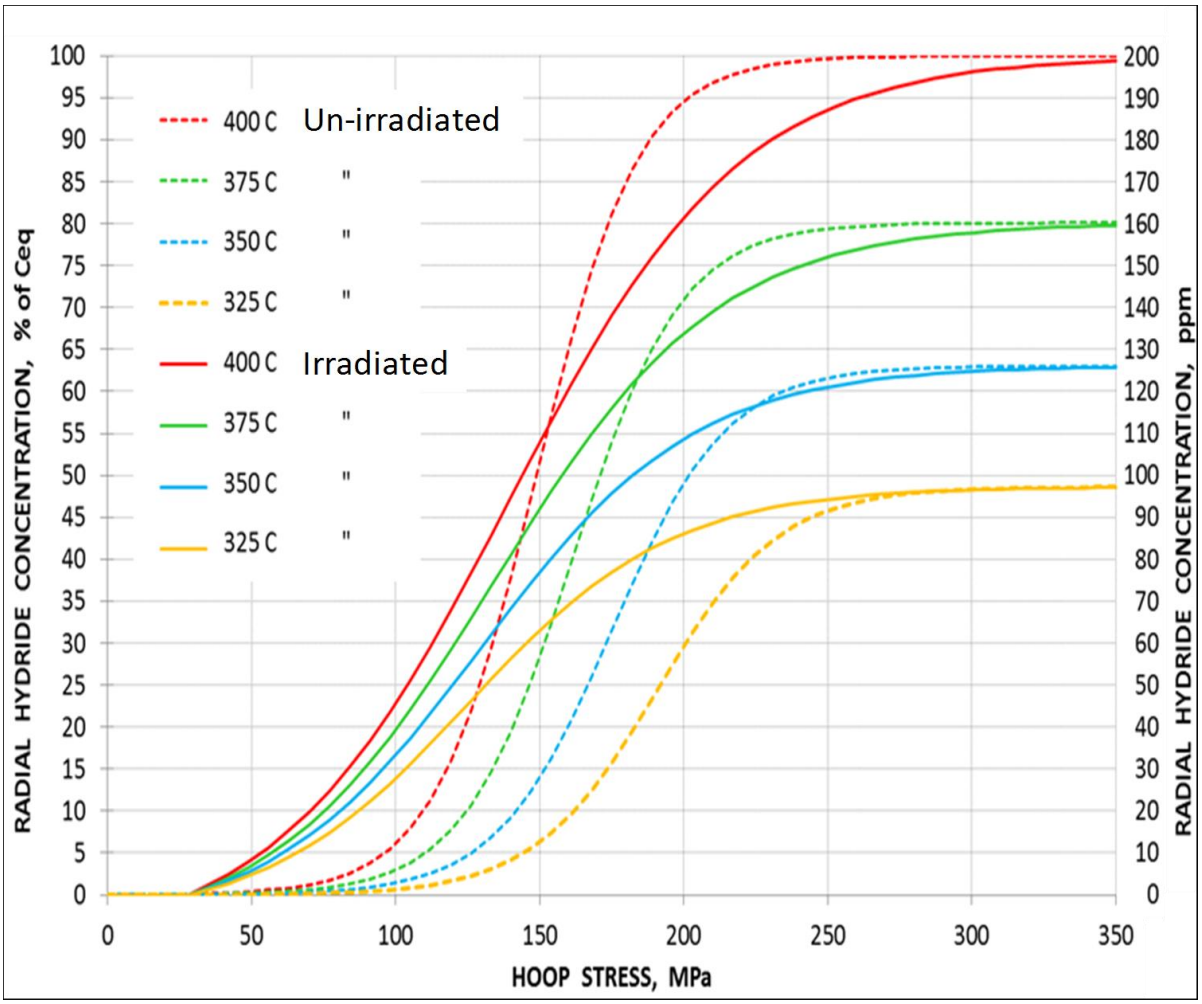

Figure 1. Model Simulation of Hydride Reorientation in Zr-4 cladding, depicting radial hydrides content as fraction of the 400° solvus (left axis), and as wppm (right axis), material Cooled under Stress from Indicated Temperature to RT [4].

While Figure 1 covers a wide range of hoop stress, the cladding hoop stress in high burnup spent fuel rods, as calculated by the pressurized-tube (open gap) formula, is in the range of 90-120 MPa. The hoop stress in fully bonded cladding should be significantly lower than the open-gap case; this will be determined by the analysis in this paper, covering only the first 60 days of dry storage, which, as will be shown, is the period of transient changes in cladding stresses before settling down to a steady state condition.

ANALYSIS APPROACH

Figure 2 shows two micrograph images of fuel-cladding bonding at high burnup typically seen during PIE [5]. The analysis approach employs finite element representations of these two cross-sections as representative configurations of high burnup, bonded fuel rods with a fractured/fragmented pellet. These images represent bounding conditions for high-burnup fuel, where the left image represents pellet cracks that remain confined to the

interior of the pellet, and the right image represents pellet cracks that extend to the pellet-cladding interface. Clearly, a combination of these two configurations can exist; however, the two crack configurations include sufficient variation to make the calculated cladding stresses typically representative of the majority of high-burnup spent fuel rods in dry storage.

The fuel rod void volume in which the gas resides consists of crack volumes and fuel matrix open porosity and micro-cracks, which are invisible to the naked eye. The gas is assumed to conform to the ideal gas law during the temperature rise that occurs during the drying process.

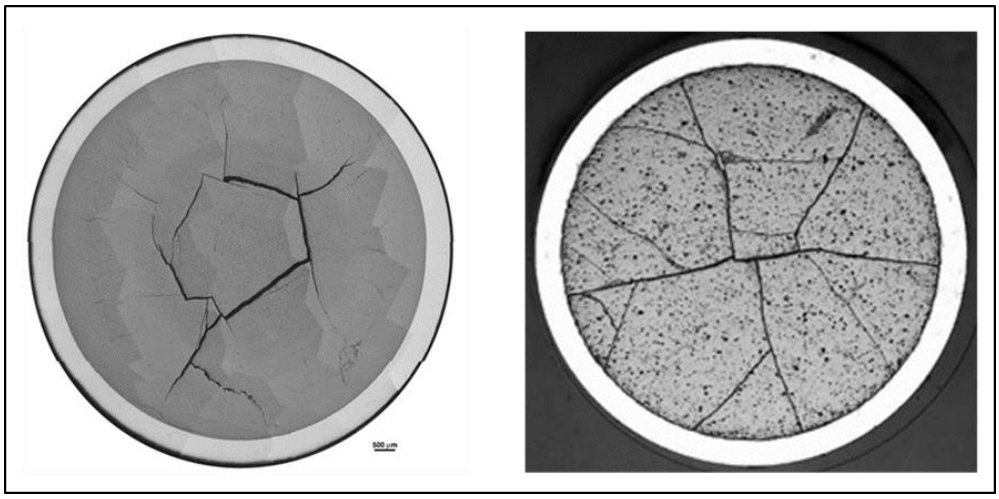

Figure 2. Examples of bonded fuel-cladding with fractured/fragmented fuel pellets. Pattern-1 left: Limited cracking without reaching pellet-cladding interface. Pattern-2 right: More extensive cracking with crack tips at the pellet-cladding interface.

Two finite element models (FEM), representations of the Figure-2 images, are shown in Figure 3: a) an internal crack pattern, (Pattern-1, representing Figure 2 left), and b) a more extensive crack pattern, (Pattern-2, representing Figure 2 right). The fuel performance analyses were conducted using the BISON fuel performance code [6], which is a three-dimensional finite-element-based fuel behavior code. The cross sections shown in Figure 3 are assumed to be in a state of plane strain, which is compatible with full length fuel rod response.

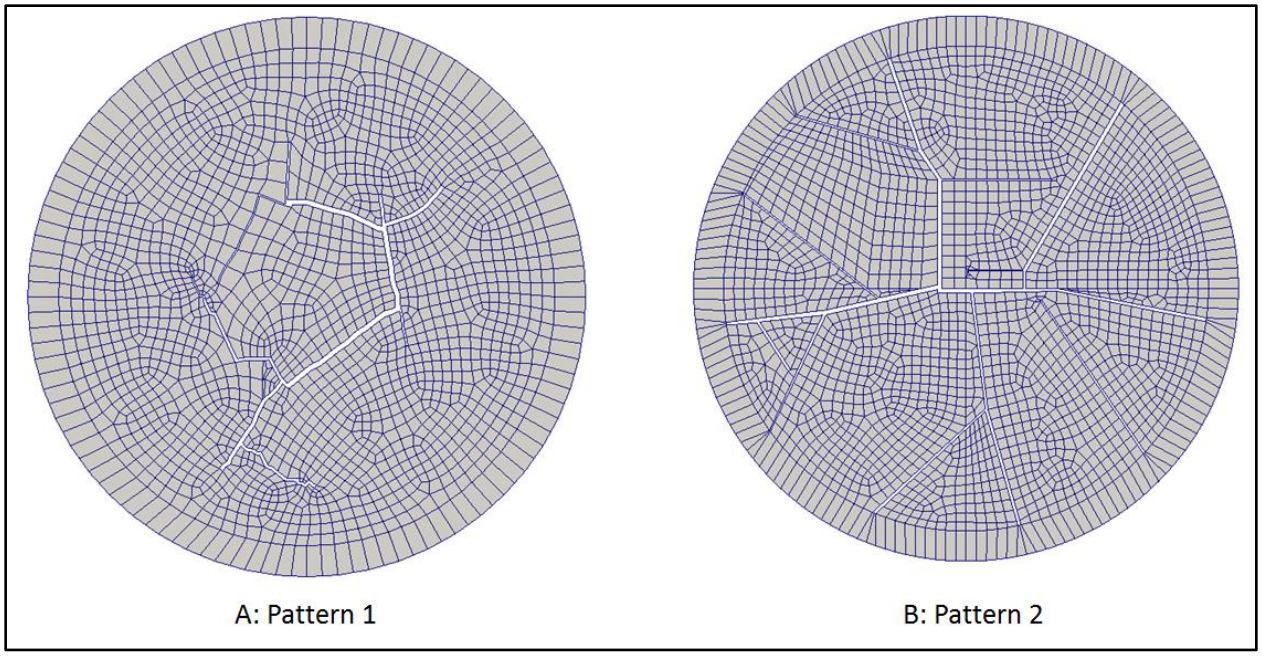

Figure 3. Finite element analysis models of the images in Figure 2.

An important consideration in the analysis process is defining a realistic value for the maximum temperature reached during vacuum drying, which is likely to be significantly lower than the regulatory limit of 400ºC because the energy level in spent fuel assemblies is not sufficient to cause the fuel temperature to rise to such high levels during vacuum drying. Recent spent fuel dry storage cask thermal modeling and temperature measurements have confirmed this condition. To address the consideration of a lower vacuum drying temperature, the analysis was performed considering two possible limits for the vacuum drying temperature, 400ºC and 350ºC, and two complete sets of analysis results are presented in this paper. Detailed discussion will focus on the 400ºC case, but equivalent results for the 350ºC case are included in the Appendix. To facilitate direct visual comparison, the figure numbers for the 350ºC case were kept the same as the 400ºC figures but with the letter A, for Appendix, added.

Establishing Initial Conditions

In the present simulation, the end of life quantities of burnup, fast fluence, and internal rod pressure were input to the models as the initial conditions for the start of vacuum drying. The initial burnup, fast fluence, and internal rod pressure were set to 59.02 GWd/tU, 9.0×10^{25} n/m^2, and 4.95 MPa [7] prior to the start of vacuum drying, respectively.

Simulation of Vacuum Drying

The vacuum drying process was simulated by applying a constant decay power value of 1 W/m consistent with typical discharge burnup, (1-2 kW/assembly), and adjusting the cladding surface heat transfer coefficient to induce a cladding temperature increase from 40°C, the wet storage temperature, to 400°C, then held constant for 60 days to allow thermal creep to bring the stresses generated by differential fuel-cladding thermal expansion to come to quiescent steady state condition. The vacuum drying simulations of cladding temperature and rod internal pressure are shown in Figure 4.

The loading condition during the vacuum drying process consists of thermal expansion of both the fuel and the cladding and the temperature-dependent internal gas pressure in the discrete cracks and in the fuel matrix open porosity. The cladding stress state at the end of the 400ºC-temperature hold time is the stress condition that governs the hydride reorientation process and is used here as the metric for judging the effects of fuel-cladding bonding. This is discussed in the next section.

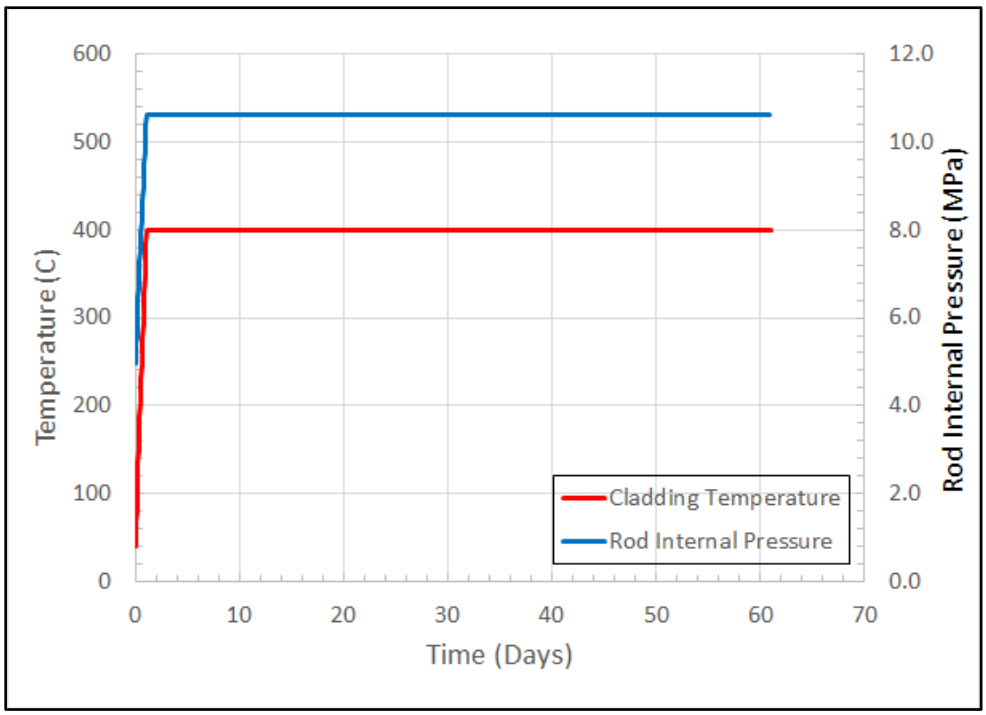

Figure 4. Cladding temperature and rod internal pressure simulations of vacuum drying.

ANALYSIS RESULTS

The thermo-mechanical analyses performed are listed in Table 1 below. Cases 1 through 8 consider the two fully bonded pellet-cladding configurations depicted in Figure 2.

Table 1. Analytical Model Cases, Peak Cladding Hoop Stress, and Model Descriptions

Case	Description
1	Fracture Pattern-1, at the start of the vacuum drying process. (Figure 5)
2	Fracture Pattern-2, at the start of the vacuum drying process. (Figure 6)
3	Fracture Pattern-1, at the completion of the vacuum drying process. (Figure 7)
4	Fracture Pattern-2, at the completion of the vacuum drying process. (Figure 8)
5	Fracture Pattern-1, just prior to the completion of the vacuum drying process. (Figure 9)
6	Fracture Pattern-2, just prior to the completion of the vacuum drying process. (Figure 10)
7	Fracture Pattern-1, after 60 days of creep in dry storage. (Figure 11)
8	Fracture Pattern-2, after 60 days of creep in dry storage. (Figure 12)

The results are depicted in a series of figures that correspond to the cases in Table 1, showing contour plots of the stress distribution in the pellet and the cladding, and a scale calibrated to indicate the magnitude of the computed stress; note that the stress components of interest are: the radial stress in the fuel which represents the pellet-cladding mechanical interaction (PCMI) force, and the hoop stress in the cladding which governs hydride reorientation.

Because of fuel-cladding differential thermal expansion, (higher in the fuel than the cladding), the vacuum drying process will activate two PCMI force components: a radial force and a tangential interfacial force, which contribute additively to the time evolution of the cladding hoop stress. These forces are absent in the un-bonded open gap case where the internal gas pressure acts directly on the cladding.

Initial Pre-Vacuum Drying Stress Distributions

Cases 1 and 2 (Figures 5 and 6) depict simulations of the initial stress conditions for dry storage, at the start of vacuum drying. These stresses represent the stress conditions at approximately 40ºC in the spent fuel pool.

Figure 5 depicts the stress distribution in the pellet and the cladding for Pattern-1 prior to subjecting the fuel to the vacuum drying process. Figure 5 shows the cladding stresses to be slightly in tension in most areas and compressive in others. . Similar behavior is shown in Figure 6 Pattern-2, but with cladding stresses slightly in tension in all areas. The stress contour plots for the fuel indicate that the magnitude of the tension at the outer surface is below the fuel's tensile strength, and is insufficient to cause a break in the fuel-cladding bond.

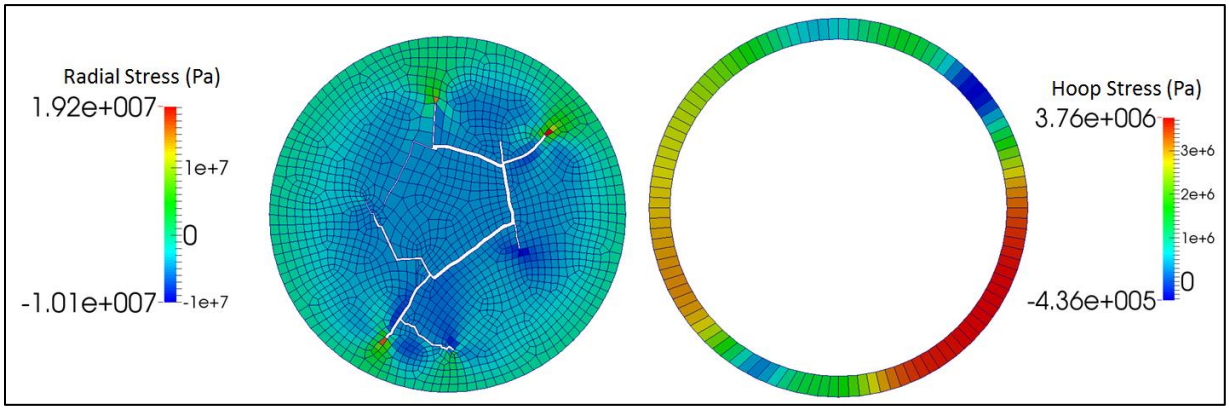

Figure 5. Case 1: Stress distribution at 40°C for Pellet-Crack Pattern-1 at the start of the vacuum drying process.

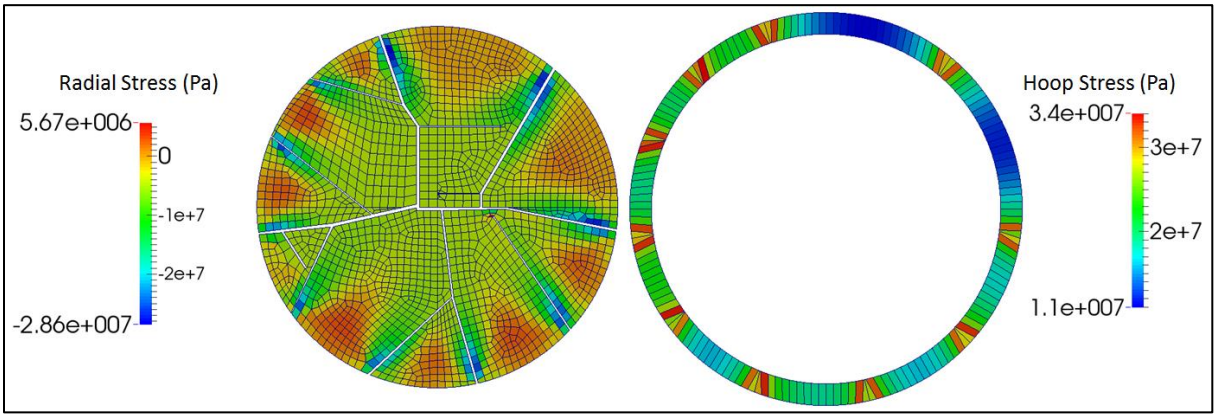

Figure 6. Case 2: Stress distribution at 40°C for Pellet-Crack Pattern-2 at the start of the vacuum drying process.

Post Vacuum Drying Stress Distributions

The stress conditions depicted in Figures 5 and 6 are reversed in Figures 7 and 8, where regions of the cladding under lower stresses before the start of vacuum drying became regions of high tension at the completion of vacuum drying. Just prior to the completion of vacuum drying at temperature of about 385ºC, peak cladding stresses of 152 MPa and 134 MPa were observed for pellet-crack Pattern-1 and Pattern-2, respectively, as shown in Figures 9 and 10. These stresses are slightly higher than the peak cladding stresses of 146 MPa and 130 MPa observed at the completion of vacuum drying shown in Figures 7 and 8. However, these high stresses are transient in nature and would be short lived because of creep and relaxation during the 60-day 400ºC temperature hold time, as will be discussed next.

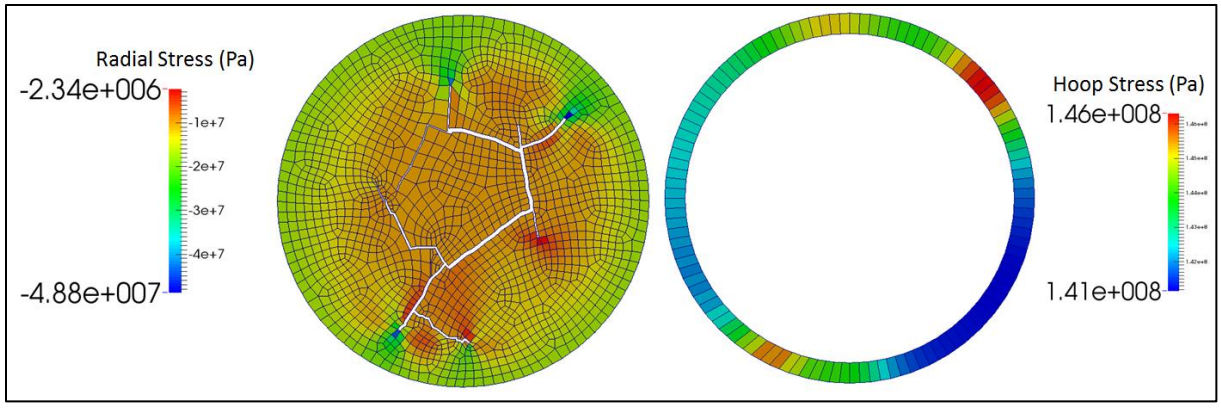

Figure 7. Case 3: Stress distribution at 400°C for Pellet-Crack Pattern-1 at the completion of the vacuum drying process.

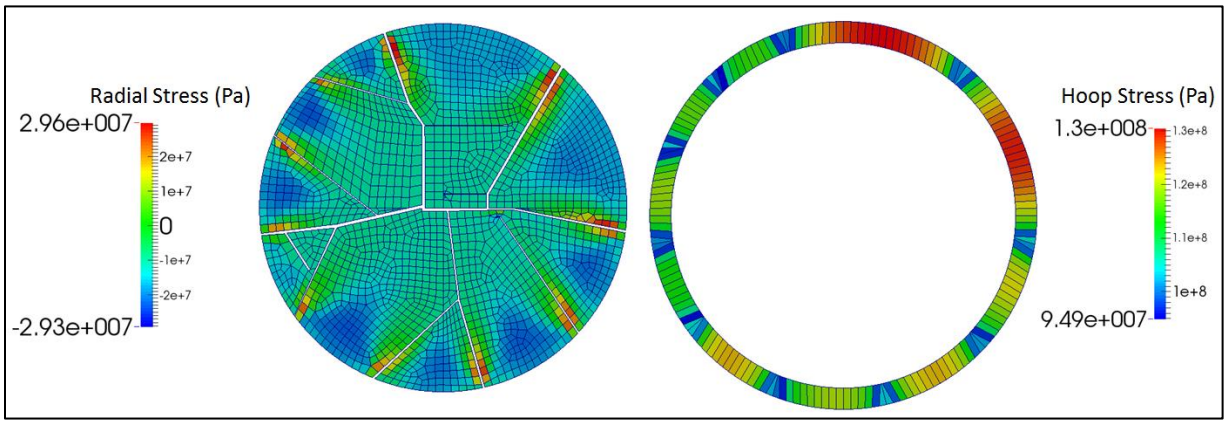

Figure 8. Case 4: Stress distribution at 400°C for Pellet-Crack Pattern-2 at the completion of the vacuum drying process.

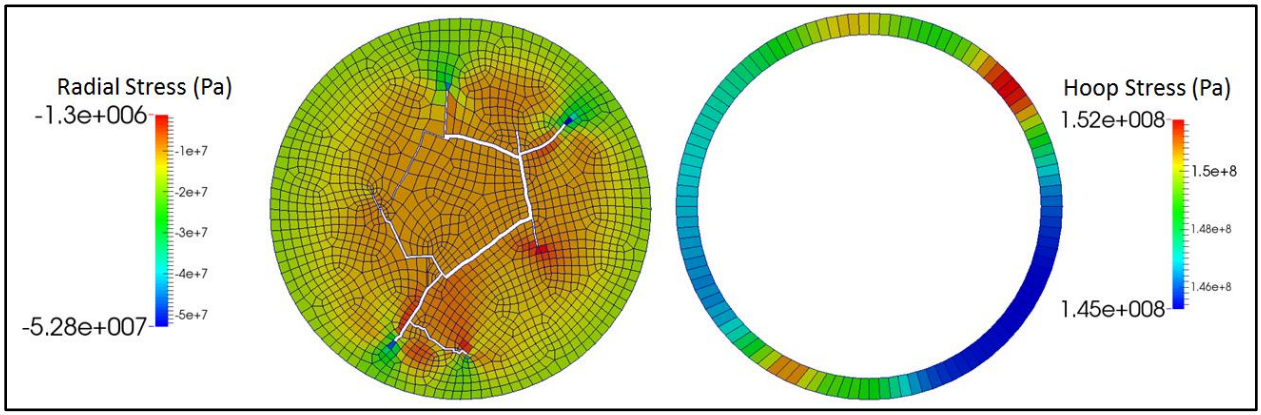

Figure 9. Case 5: Stress distribution at 385°C for Pellet-Crack Pattern-1 just prior to the completion of the vacuum drying process.

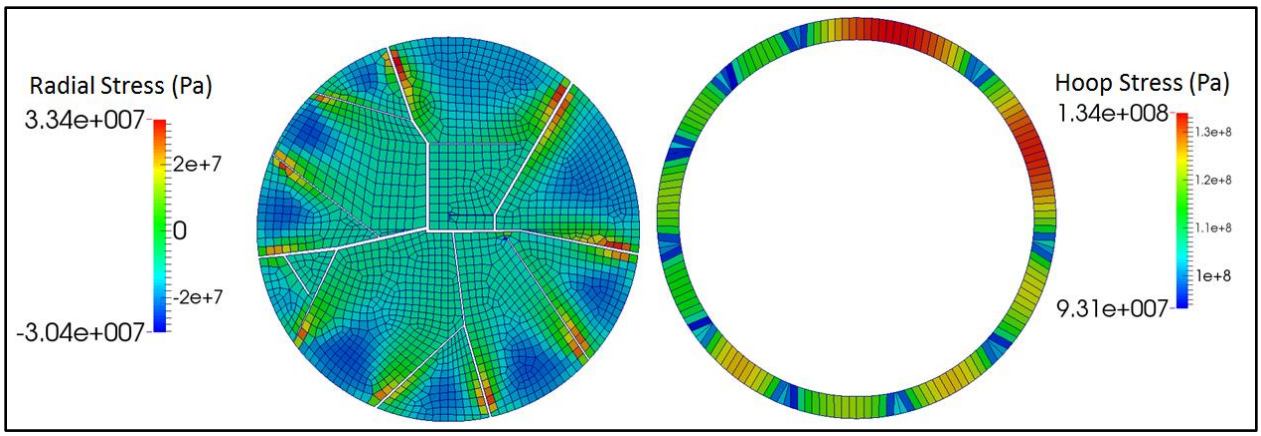

Figure 10. Case 6: Stress distribution at 385°C for Pellet-Crack Pattern-2 just prior to the completion of the vacuum drying process.

Sixty-Day Stress Distributions

Cases 7 and 8 (Figures 11 and 12) show the results after a hold time of 60 days following the completion of vacuum drying, which illustrates the effect of the relaxation of the pellet-cladding interfacial force during the 60-day 400ºC temperature hold time. This force relaxation reduces the cladding peak stress from 152 MPa (Figure 9) to 21.8 MPa (Figure 11) for Pattern-1, and from 134 MPa (Figure 10) to 67.7 MPa (Figure 12) for Pattern-2. This stress relaxation behavior is of special significance for the problem at hand and is further discussed in a later section.

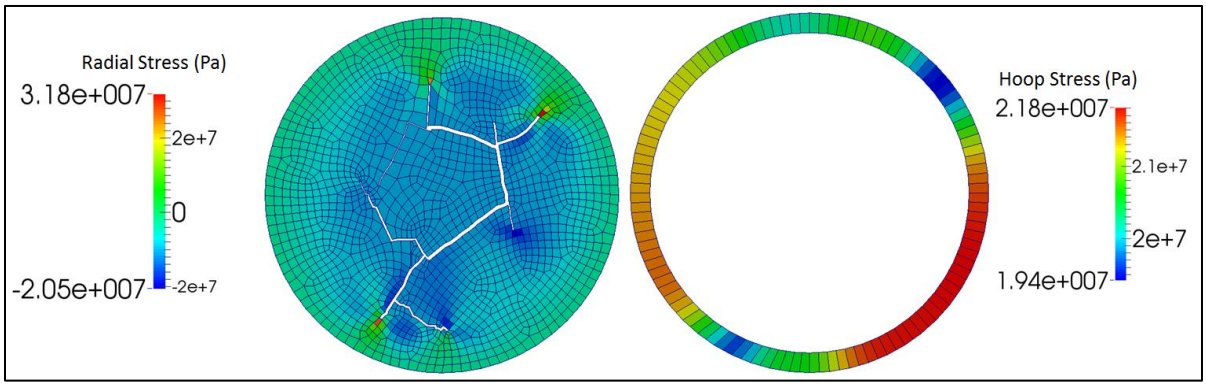

Figure 11. Case 7: Stress distribution at 400°C for Pellet-crack Pattern-1 after 60-day hold

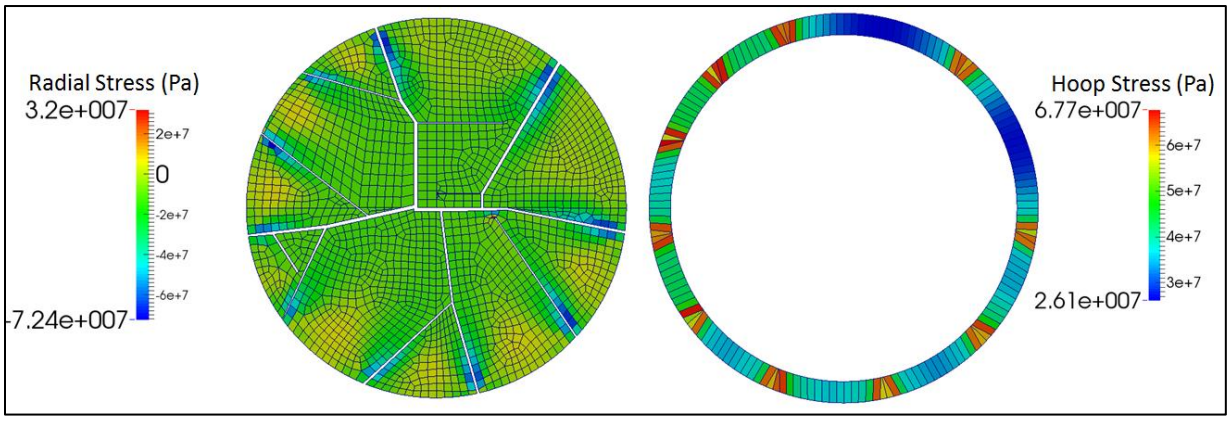

Figure 12. Case 8: Stress distribution at 400°C for Pellet-Crack Pattern-2 after 60-day hold

Effects of Creep and Relaxation on Bonded Fuel

The present study reveals that fuel-cladding bonding can be viewed as a simulation of the classical relaxation experiment in which the strain in the specimen is held fixed, while the stress is observed to relax with time. For the case at hand, the cladding is initially stretched by the differential thermal expansion and then held stationary by the non-deforming pellet. During the constant-temperature hold at 400ºC, the cladding creep rate is relatively high, but the cladding is prevented by the pellet from creeping, and to compensate for this constraint the cladding responds by relaxing its stress. This behavior is illustrated in Figure 13, which shows a rapid stress relaxation, nearly a precipitous drop within a few hours, followed by a gradual decay typical of relaxation phenomena.

The three curves in Figure 13 depict the time evolution of the peak stress anywhere in the cross section for three cases: Pattern-1, blue curve, Pattern-2 between pellet cracks, red curve, and Pattern-2 at pellet cracks, green curve. As indicated by the arrows in this figure, the between-cracks peak stress for Pattern-1 relaxed significantly from a value of 152 MPa to <22 MPa. Similarly, for Pattern-2 the between-cracks stress dropped from 134 MPa to ~27 MPa; the at-crack peak stresses for this case dropped from a value of ~106 MPa to ~55MPa, (Figure 13 green curve). These results should be contrasted with the cladding hoop stress under the open-gap assumption, which is in the range of 85 - 90MPa.

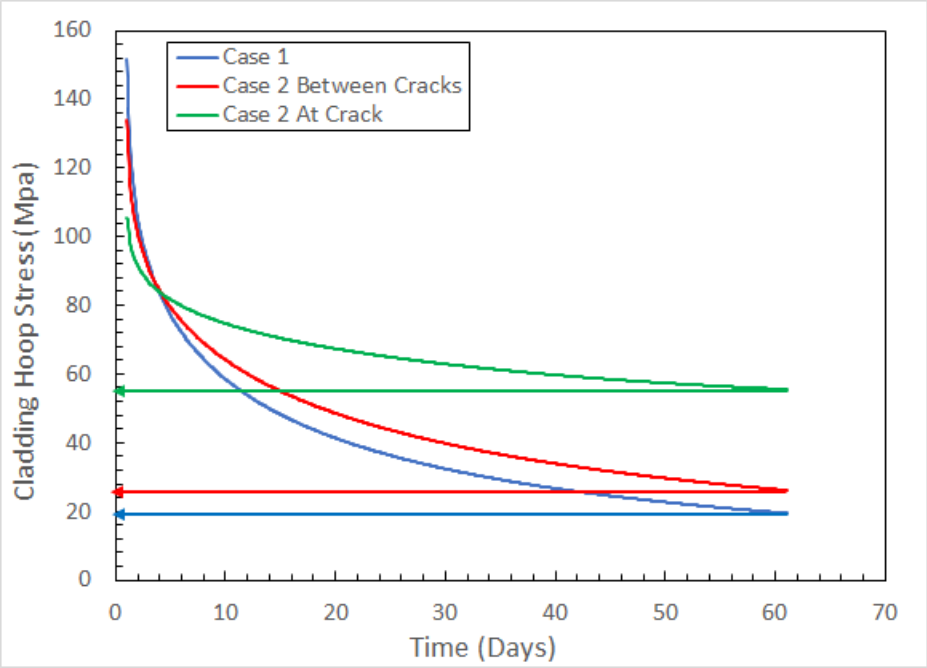

Figure 13. Evolution of cladding hoop stress during temperature hold after the completion of vacuum drying.

For easy visualization of the stress distribution in the cladding, Figures 14 and 15 show a pictorial representation of the pre-and post-creep hoop stress distributions for the two cracking patterns – it is noted that Figure 15b shows a peak stress of ~67.7 MPa instead of the ~55 MPa in Figure 13. This is due to a single element with a distorted shape, as indicated by the arrow, causing the calculations to be somewhat anomalous.

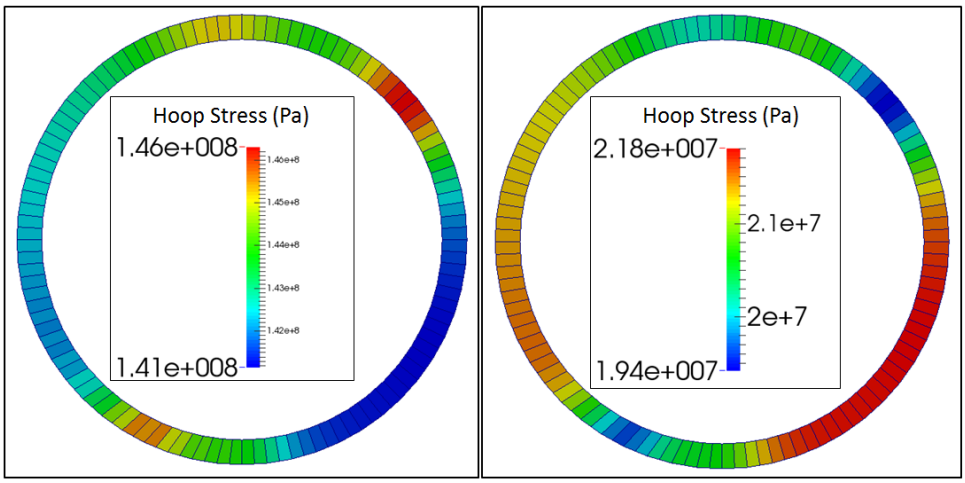

(a) Cladding hoop stress at 400ºC at zero hold time. (b) Cladding hoop stress at 400ºC after 60-day hold.
Figure 14. Case 1 Cladding hoop stress relaxation during 60-day temperature hold at 400ºC after vacuum drying.

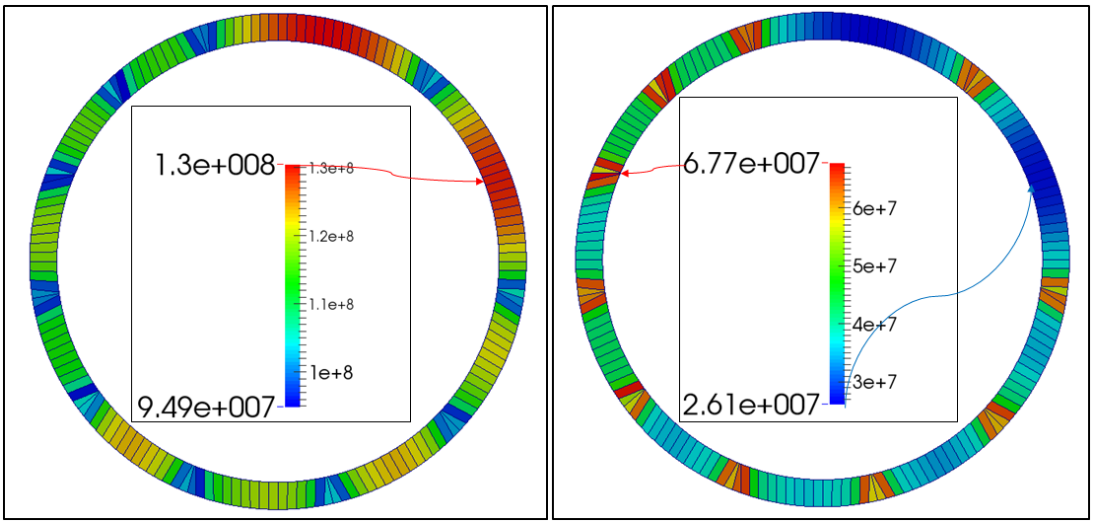

(a) Cladding hoop stress at 400ºC at zero hold time. (b) Cladding hoop stress at 400ºC after 60-day hold.
Figure 15. Case 2 Cladding hoop stress relaxation during 60-day temperature hold at 400ºC after vacuum drying.

CONCLUSION

The present study clearly indicates that high burnup fuel rods with pellet-cladding bonding follow very different behavior regimes from the pre-conceived regimes of pressurized empty tubes. The present analysis reveals several results that are not known using the traditional approach:

- High burnup spent fuel rods with fuel-cladding bonding begin their dry storage life with a state of stress that is highly non-uniform and is higher than is calculated based on the open gap assumption. However, those initial stresses are very short lived and undergo very rapid relaxation due to the high creep rate of the cladding and the pellet constraint imposed on the cladding by the bonding condition.
- Fortuitously, creep is found to be highly beneficial, unlike initial regulatory perception of creep being a limiting failure mechanism for dry storage. The analysis shows that the relaxation process reduces the cladding hoop stress to less than half the magnitude of the pressurized empty-tube formula within a time duration of a few days, although the analysis was carried out to a period of 60 days to allow steady state

conditions to develop. However, this was found to be too short for stress relaxation to cease, and further reduction would be expected. The temperature was kept constant at 400ºC for the duration, but the very small reduction in temperature due to changes in decay heat would not invalidate the results. Also, there is no possibility of hydride reorientation during the 60-day period because the temperature remains above the precipitation solvus.

- As can be seen in the stress distribution figures, the hoop stress can vary by a factor of 10 around the circumference in the between-cracks segments, with higher stress concentrations occurring in very narrow regions at pellet cracks. Even if these stress patterns are maintained during the hydride precipitation phase, one would expect that radial hydride distributions would follow similar patterns; however, the radial hydride content would be small because of the low stress.
- An overall assessment of the results indicate that high-burnup bonded fuel appears to be more trouble-tolerant than low burnup un-bonded fuel because the cladding stress state in the bonded fuel rod is lower (~68 MPa, see Figure 15) than that typically present in un-bonded rods (90 – 120 MPa) resulting in lower radial hydride concentrations (see Figure 1).

Future analysis will include studies of the effects of partial de-bonding on the cladding hoop stress in comparison to the open gap condition and the effects of in-reactor pre-shutdown condition where a state of fuel-cladding bonding had already existed at the end of burnup life to quantify the fuel and cladding initial states of stress for dry storage. Also, additional crack patterns, including circumferential cracks, will be investigated.

ACKNOWLEDGMENT

The work described in this paper was supported by the Electric Power Research Institute under contract MA 10005361 and MA 10007432 A1.

REFERENCES

1 K. Nogita and K. Une, "Formation of Pellet-Cladding Bonding Layer in High Burnup BWR Fuels," *Journal of Nuclear Science and Technology*, **Vol. 34**, No. 7, p. 679-686 (July 1997).

2 M.C. Billone, T.A. Burtseva, and R.E. Einziger, "Ductile-to-brittle transition temperature for high burnup cladding alloys exposed to simulated drying-storage conditions," *Journal of Nuclear Materials*, **433** (2013) 431-448.

3 Nuclear Regulatory Commission 2003 Interim Staff Guidance (ISG)-11, Revision 3, Cladding Considerations for the Transportation and Storage of Spent Fuel, November 2003 (ML0033230335 at: http://www.nrc.gov/readingrm/adams.html).

4 W. Liu, J. Rashid, and A. Machiels, "A Hydride Reorientation Model for Irradiated Zirconium Alloy Cladding", TopFuel-2016, EPRI-3002002969, Technical Update, June 2014.

5 A. Machiels, Session 4: Technical Issues Cladding Presentation, 2015 Division of Spent Fuel Management (DSFM) Regulatory Conference, Washington, DC, November 18-19, 2015, http://www.nrc.gov/public-involve/conference-symposia/dsfm/2015/dsfm-2015-albert-machiels.pdf

6 J. D. Hales, K. A. Gamble, B. W. Spencer, S. R. Novascone, G. Pastore, W. Liu, D. S. Stafford, R. L. Williamson, D. M. Perez, R. J. Gardner, BISON Users Manual: BISON Release 1.2, Technical Report INL/MIS-13-30314 Rev. 2, Idaho National Laboratory, September 2015.

7 A. Machiels, "End-of-Life Rod Internal Pressures in Spent Pressurized Water Reactor Fuel", EPRI Report 3002001948, Technical Update, December 2013.

Appendix – Results for the Case of 350ºC Vacuum Drying Temperature

This appendix conttains the figures for the 350ºC vacuum drying temperature, with the figure numbers kept the same as for the 400ºC temperature to facilitate comparison. An interesting difference between the two sets of figures is the effect of the lower creep rate on stress relaxation, resulting in somewhat higher terminal stresses for Pattern-2 cases, and significantly higher stress for Patern-1. This implies that lower-energy spent fuel would be more, at least equally, vulnerable to hydrides reorientation. The peak cladding stresses of 147 MPa and 129 MPa were observed to be at the completion of vacuum drying process for both pellet-crack Pattern 1 and Pattern 2, respectively, relaxing down to 83 MPa after 60 days. The corresponding values for the 400ºC case are: 146 MPa and 130 MPa, relaxing down to 22 MPa and 68 MPa. Using these stresses, radial hydrides can be estimated from Figure A-1. This is determined from the

figure below to be ~20 ppm and ~25 ppm, respectively, for the two stress-temperature pairs of (400ºC, 68 MPa) and (350ºC, 83 MPa). The 5 ppm difference in radial hydrides may not be significant, but it demonstrates that a reduced initial storage temperature does not necessarily mean a better choice.

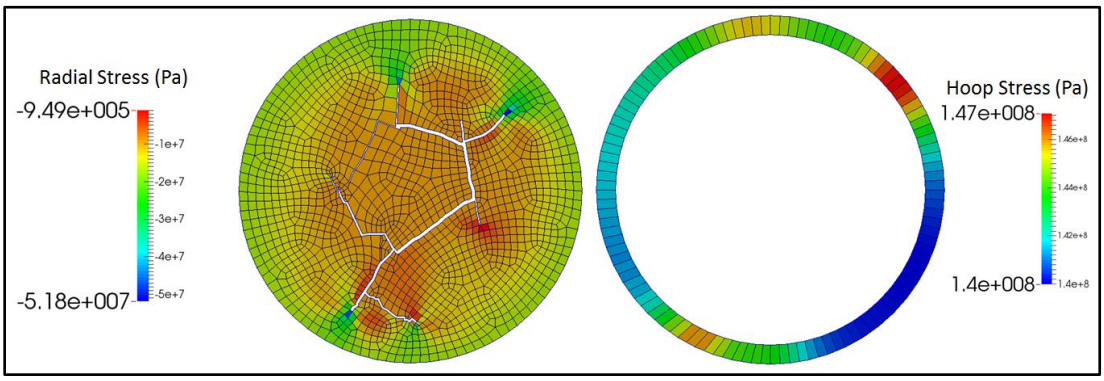

Figure A-7. Case 3: Stress distribution at 350°C for Pellet-Crack Pattern-1 at the completion of the vacuum drying process.

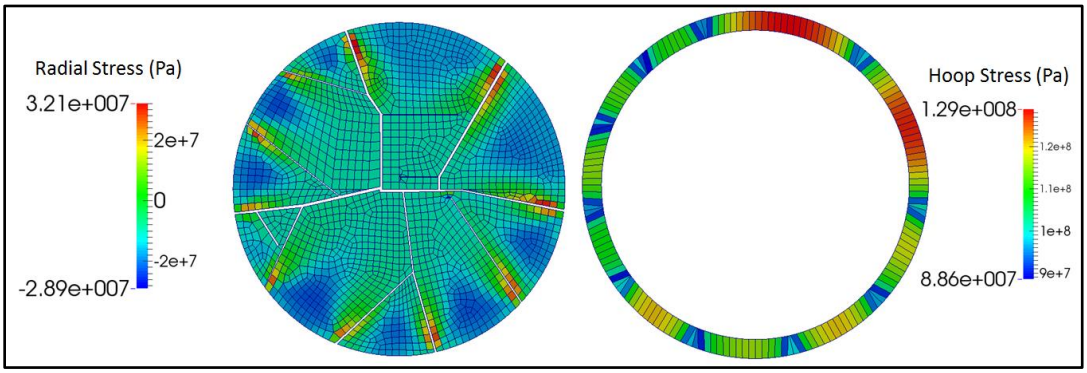

Figure A-8. Case 4: Stress distribution at 350°C for Pellet-Crack Pattern-2 at the completion of the vacuum drying process.

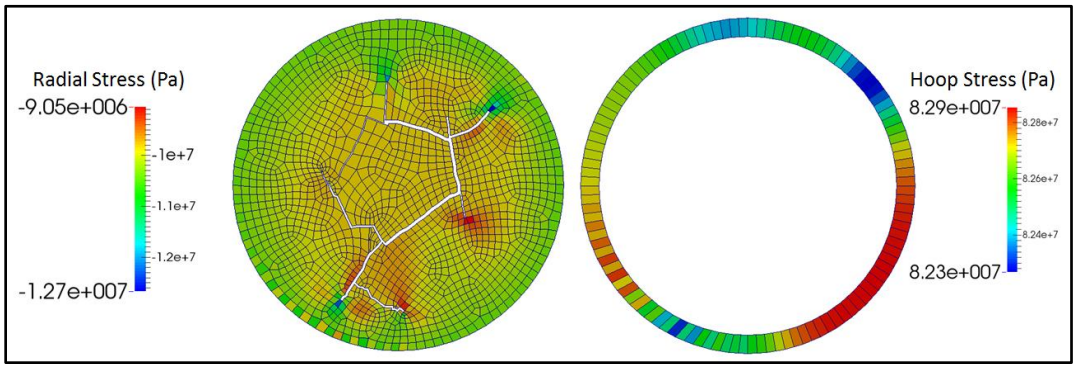

Figure A-11. Case 5: Stress distribution at 350°C for Pellet-crack Pattern-1 after 60-day hold

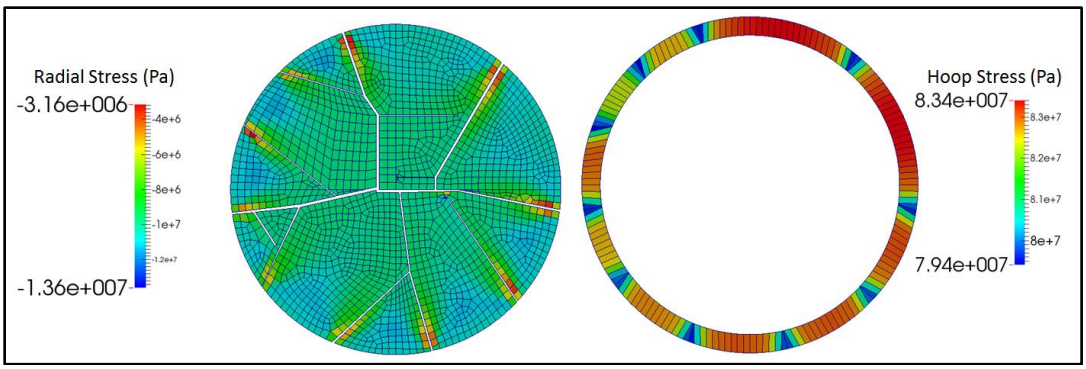

Figure A-12. Case 6: Stress distribution at 350°C for Pellet-Crack Pattern-2 after 60-day hold

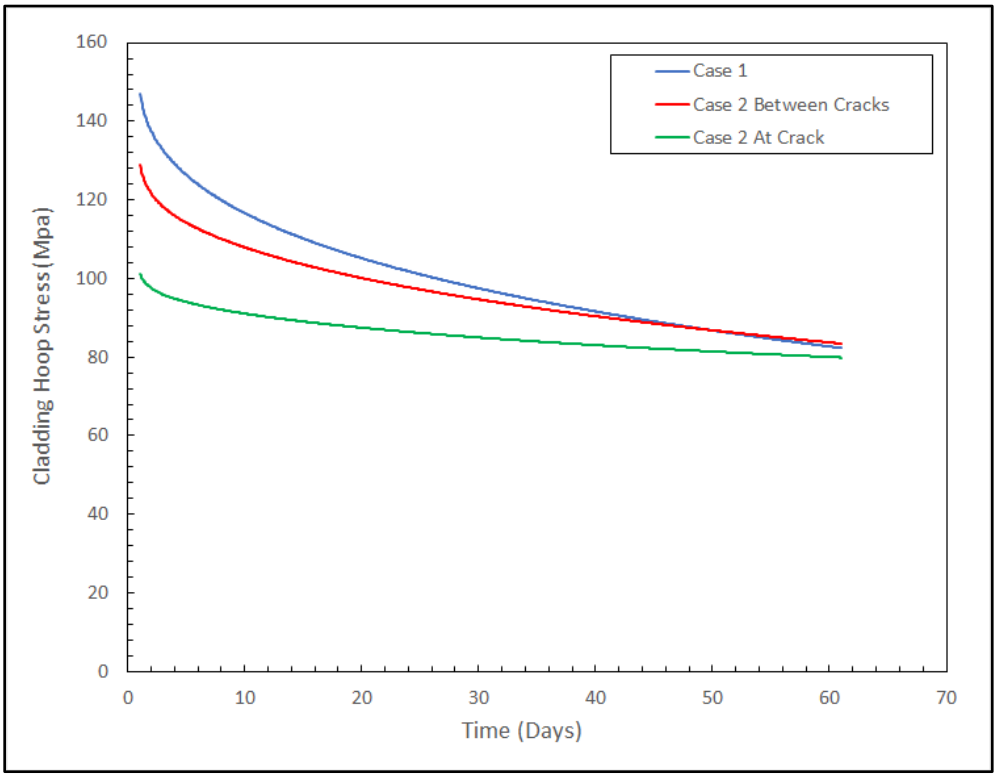

Figure A-13. Evolution of cladding hoop stress during temperature hold after the completion of vacuum drying.

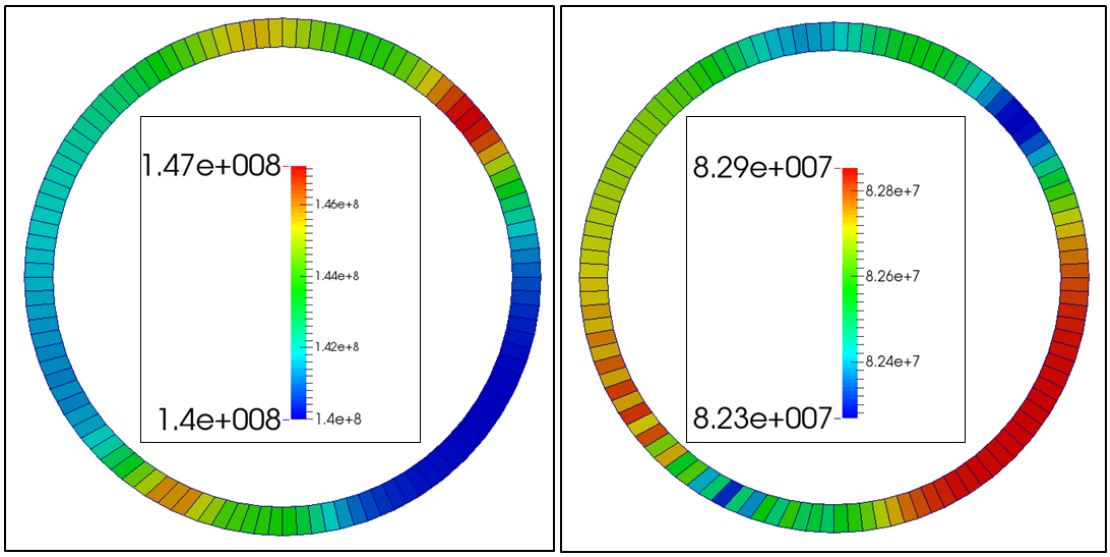

(b) Cladding hoop stress at 350ºC at zero hold time. (b) Cladding hoop stress at 350ºC after 60-day hold.
Figure A-14. Case 1 Cladding hoop stress relaxation during 60-day temperature hold at 350ºC after vacuum drying.

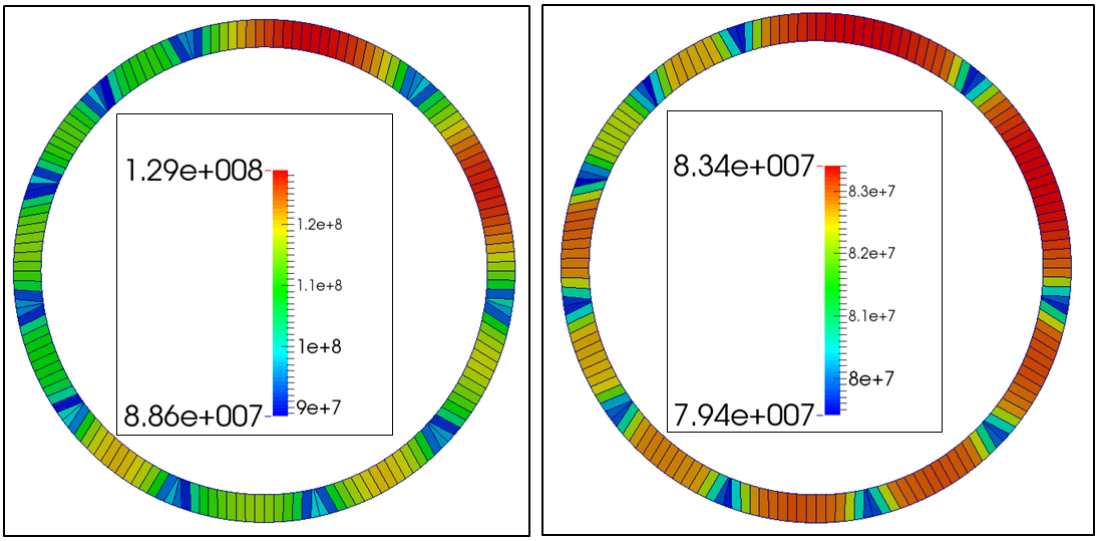

(b) Cladding hoop stress at 350ºC at zero hold time. (b) Cladding hoop stress at 350ºC after 60-day hold.
Figure A-15. Case 2 Cladding hoop stress relaxation during 60-day temperature hold at 350ºC after vacuum drying.

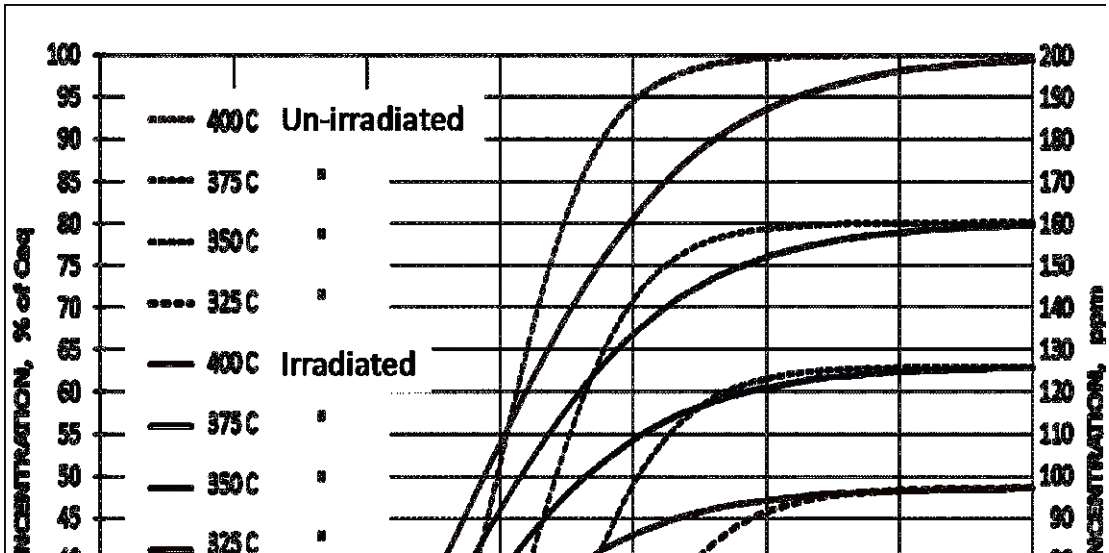

Figure A-1. Model Simulation of Hydride Reorientation in Zr-4 cladding – a Duplicate of Figure 1.